The Implementation of Simplified Simple Biosphere (SSiB) Scheme in the Regional Spectral Model (RSM)

Vasubandhu Misra[#], Paul A. Dirmeyer, Ben P. Kirtman

Center for Ocean-Land-Atmosphere Studies
Institute of Global Environment and Society, Inc.
4041 Powder Mill Road, Suite 302
Calverton, MD 20705.

Corresponding author

E-mail: misra@cola.iges.org

March 2001

Abstract

The Simplified Simple Biosphere (SSiB) scheme of Xue et al. (1991) and Dirmeyer and Zeng (1997) is coupled to the atmospheric Regional Spectral Model (RSM). The coupling ensures that mass in the coupled land-atmosphere model is conserved. Besides the fluxes the RSM ingests the surface roughness and drag coefficient for the momentum flux. SSiB uses the large scale and convective precipitation, shortwave and down-welling longwave fluxes at the surface, specific humidity, dry temperature, wind speed at the lowest sigma level, solar zenith angle and the rain/snow flag based on the 850 hPa temperature of the RSM.

In this study we find that the coupled land atmosphere integration using the SSiB scheme improves the seasonal simulation of precipitation over the South Atlantic Convergence Zone (SACZ) relative to the control version of the model which contains a two layer soil model with uniform vegetation fraction. Furthermore a relative improvement in the seasonal simulation of surface temperature over the Amazon river basin is also seen from RSM runs coupled to SSiB. However, the RSM-SSiB runs exhibit a strong warm bias in the surface temperature over the sub-tropics of South America. There are some significant changes in the low level circulation simulated by both models, which however produce very similar interannual variability in the low level jet to the east of the Andes.

1. Introduction

This is a sequel to a recent paper on regional climate simulation over South America (Misra et al. 2000, hereafter M2000). In the earlier paper we used the control version of the Regional Spectral Model (RSM) following Juang and Kanamitsu (1994). Since then we have implemented the Simplified Simple Biosphere (SSiB) scheme following Xue et al. (1991), Dirmeyer and Zeng (1999) as an alternative land surface parameterization in the RSM to the existing land surface scheme of Mahrt and Pan (1984). Our interest in using a more sophisticated land surface scheme in regional climate modeling stems from recent studies which have shown a significant impact of land surface processes on the predictability of precipitation on seasonal to interannual scales (Fenessey and Shukla 1996, Paegle et al. 1996). Many of these modeling studies have shown the importance of the soil wetness on the evolving climate. Dirmeyer (2000a), Viterbo and Betts (1999) using initial soil moisture initial conditions calculated offline by forcing a 2-D version of the same land surface scheme as the GCM with analyses of near surface meteorological conditions showed substantial improvement in the climate anomalies generated from the GCM. Furthermore recent studies have shown that critical relationships between the soil moisture and the surface fluxes are well captured by the more advanced land surface schemes (Dirmeyer et al. 2000b).

The SSiB scheme developed first by Sellers et al. (1986) and later simplified by Xue et al. (1991) is one of the many complex land surface schemes in existence now. One of the main motivating factors to chose this scheme over others is that we want to make the physics of the RSM as compatible as possible to the physics package in the Center for Ocean-Land-Atmosphere General Circulation Model (COLA GCM), which we intend to use to provide the lateral boundary conditions to drive the RSM. Moreover this scheme is well tested in the COLA GCM (e.g. Fenessey et al. 1994a, 1994b, 1996).

The current AGCM lacks the horizontal resolution to resolve regional orographically forced

precipitation and fine scale synoptic and meso-scale systems which contribute significantly to the local climate. The current computing resources preclude the increase of the horizontal resolutions of the AGCM to very fine scales. An alternative approach that the community has adopted is the use of limited area models nested within the coarser grid resolution of the AGCM. The increased horizontal resolution of the regional climate model has shown great promise in addressing seasonal predictability issues over western U.S. (Giorgi, 1990), over the Indian monsoon region (Ji and Vernekar, 1997), and over the South American region (M2000, Tanajura et al. 1996, Chou et al. 2000). M2000 show that the RSM is able to enhance the information content at intra-seasonal (30-60 days) and higher frequency (3-30 days) scales over the South American region relative to the coarser National Center for Environmental Prediction (NCEP) reanalysis.

One of the other reasons to undertake this work was that South America has a considerable spatial heterogeneity in the vegetation and soil types which could influence the local climate. In Fig. 1 we depict the map of vegetation types over the South American continent derived from the International Satellite Land Surface Climatology Project (ISCLP). The figure shows that there is enough heterogeneity in the vegetation type to warrant an investigation of its effect on the regional climate. Preliminary work of Pereira et al. (2000) suggest that over Rondonia in central Amazon the first appearance of shallow cumulus clouds on convective days was over forested areas while there is a bias for cumulus growth over deforested areas during the dry season (July-October). In addition, they mention that the deeper clouds with higher reflectivity values form in areas where the forest neighbours pasture areas.

In the following section, we shall briefly describe the two land surface schemes which are coupled to the atmosphere of the RSM, followed by a detailed description of the coupling of the SSiB scheme to the atmosphere. The readers are referred to Juang and Kanamitsu (1994, 1997), M2000 for details on the RSM. The results are presented in section 4 followed by conclusions in

section 5.

2. Model Description

a) SSiB Model

The SSiB is based on a simplification (Xue et al. 1991, 1996) of the Simple Biosphere Scheme (SiB) proposed by Sellers et al. (1986). This simplification entailed the reduction of vegetation layers from two to one with ground cover vegetation being removed, simplified stomatal resistance on root-zone soil wetness and the parameterization of the fluxes of heat and water between canopy and the adjacent atmosphere using a linearized version of the Monin-Obukhov theory. However, the full two stream calculation for surface radiation (Sellers, 1985) has been retained (Dirmeyer and Zeng 1997, 1999). The SSiB has 8 prognostic variables in canopy air space temperature, two (top and deep) soil temperatures, three soil moisture stores and two interception water stores in the canopy and ground.

From the atmospheric model (RSM), SSiB receives temperature, vapor pressure and wind speed at the lowest sigma level of the RSM, precipitation rate, solar zenith angle, the rain/snow flag (based on the temperature at 850 hPa), short wave and down-welling long wave radiation flux at the surface. The SSiB communicates back to RSM sensible and latent heat fluxes, and roughness and drag coefficient for momentum fluxes.

The fluxes in SSiB are determined as a ratio of potential difference to resistance. There are three aerodynamic resistances corresponding to the resistance between the soil surface and canopy air space, the resistance between canopy leaves and canopy air space, and the resistance between canopy air space and reference height. These resistances are obtained as a function of the morphology of vegetation, soil type, wind speed and corresponding potential difference of temperature. Additionally, two more resitances, viz., bulk stomatal resistance and bare soil surface resistance, are imposed to the flux of water vapor from the upper soil layer and from within the canopy to the

adjacent air. The readers are referred to Sellers et al. (1986) for the details of these resistances. The latent (sensible) heat fluxes in SSiB which are communicated to the atmospheric model are determined as the ratio of the potential difference of vapor pressure (temperature) between the canopy source height and the reference level (lowest sigma level of the RSM) to the corresponding resistance. The spatially varying soil parameters and spatio-temporally varying vegetation parameters are prescribed from the International Satellite Land Surface Climatology Project (ISLSCP) Initiative I land surface data set (Meeson et al. 1995).

The interception, reflection, transmission and absorption of radiation by the canopy and ground are handled by the "two stream method" in SSiB. This method incorporates the incident radiation in 5 components viz., visible (diffuse and direct), near infrared (diffuse and direct) and thermal infrared (diffuse only). The method also allows for multiple reflection of light by leaves.

b) Control Soil Model

The soil moisture model of Mahrt and Pan (1984) is a two layer model. It consists of a thin upper layer of 5 cm. thick and a thicker lower layer of 95 cm. Surface evaporation and the response to diurnal variations are related to soil moisture near the surface while storage of soil water and transpiration are related to soil moisture in the deeper layer. The hydraulic conductivity and diffusivity are not properties of the soil but rather functions of soil moisture profile near the surface. Any precipitation which cannot infiltrate or re-evaporate is specified to be runoff. There are five prognostic equations corresponding to the soil moisture content, soil temperature at surface and deep layer of soil and an equation for the canopy water content. The vegetation fraction is assumed to be constant at 0.7 and soil type does not vary spatially. The surface boundary conditions for the soil water content and temperatures are the corresponding fluxes, while deep layer drainage and prescribed deep soil temperature are the bottom boundary conditions respectively.

The coupling of the land surface schemes is explicit. The previous atmospheric conditions

and updated surface variables are used in solving the surface energy balance equation (Polcher et al. 1998). To remove occasional large amplitude oscillations in surface and soil temperatures we adopt the time filtering technique of Kalnay and Kanamitsu (1988).

3. Vertical diffusion of SSiB fluxes in RSM

The turbulence diffusion equation is given by:

$$\frac{\partial A}{\partial t} = \frac{\partial}{\partial z}\left[K_A\left(\frac{\partial A}{\partial z} - \gamma_A\right)\right] \tag{1}$$

where, K_A is the diffusion coefficient and γ_A (counter- gradient term) is a correction to the local gradient that incorporates the contribution of the large-scale eddies to the total flux. A corresponds to the prognostic variables of the RSM which include u, v, θ and q (see table 1 for the meaning of symbols). This equation is solved following Hong and Pan (1996). In this procedure, first the planetary boundary layer (PBL) height is determined followed by the computation of the diffusion coefficient. Finally the diffusion equation (1) is solved to obtain the local tendency.

a) Determination of PBL height

A first guess of PBL height is determined as the lowest level where $R_{iB} > R_{iBcr}$ where,

$$R_{iB} = \frac{g h_{pbl}\left(\theta_v(h_{pbl}) - \theta_{vr}\right)}{\theta_{vr}\left|U(h_{pbl})\right|^2} \tag{2}$$

and $R_{iBcr} = 0.5$

Next, profile functions for momentum (ϕ_m) and for the thermodynamic variables T and q (ϕ_T) are computed:

For unstable and neutral conditions,

$$\phi_m = \left(1 - 16\frac{0.1 h_{pbl}}{L}\right)^{\frac{-1}{4}} \tag{3}$$

$$\phi_T = \left(1 - 16\frac{0.1 h_{pbl}}{L}\right)^{\frac{-1}{2}} \tag{4}$$

For stable conditions,

$$\phi_m = \phi_T = \left(1 + 5\frac{0.1h_{pbl}}{L}\right)^{\frac{-1}{4}} \tag{5}$$

where, L is given by:

$$L = \frac{\rho C_p \theta_{sfc} u_*^3}{kg\left(\overline{w'\theta'}\right)_{sfc}} \tag{6}$$

Here, the vertical eddy flux of potential temperature is obtained from SSiB (as sensible heat flux) in the coupled model.

Next, the mixed layer velocity scale is computed as

$$w_s = 7.8\frac{u_*}{\phi_m} \tag{7}$$

Here, u_* is specified over land points from SSiB and w_s is bounded: $\frac{u_*}{16} \leq w_s \leq \frac{u_*}{5}$ ms^{-1}. The counter-gradient terms are then computed only when $R_{iBsfc} > 0$ and the sum of latent and sensible heat fluxes are greater than zero. Here,

$$R_{iB} = \frac{g\delta z_1\left(\theta_{vr} - \theta_{vsfc}\right)}{\frac{\left(\theta_{vr}+\theta_{vsfc}\right)}{2}\left|U(z_1)\right|^2} \tag{8}$$

and then γ_A is computed:

$$\gamma_A = 7.8\frac{\overline{w'A'}}{w_s} \tag{9}$$

Over land points the flux is specified from SSiB. The counter-gradient terms are bounded as follows: $0 \leq \gamma_T \leq 3$ km^{-1} and $0 < \gamma_q < .002$ km^{-1}.

Next the thermal excess, which is the scaled virtual temperature excess near the surface, is computed as:

$$\theta_T = \gamma_T + \left(\frac{R_v}{R_d} - 1\right)\theta_{sfc}\gamma_q \tag{10}$$

Under weak wind conditions, θ_T can become very large and so it is bounded within $0^0 < \theta_T < 3^0$. A new PBL height is determined again as the lowest level where $R_{iB}^n > R_{iBcr}$, where superscript 'n' refers to a new estimate:

$$R_{iB} = \frac{g h_{pbl} \left(\theta_v(h_{pbl}) - (\theta_{vr} + \theta_T)\right)}{\theta_{vr} |U(h_{pbl}|^2} \tag{11}$$

b) Computation of diffusion coefficient

After computing the PBL height, the diffusion coefficient in the mixed layer and the free atmosphere is determined.

i) In the mixed layer

The diffusion coefficient in the mixed layer is computed using the non-local K approach. The Prandtl number is determined as:

$$P_r = \frac{\phi_h}{\phi_m} + 0.78k \tag{12}$$

The diffusion coefficient for momentum in the mixed layer is then obtained as:

$$K_m(z) = k w_s z (1 - \frac{z}{h_{pbl}})^2 \tag{13}$$

and diffusion coefficients of temperature (K_T) and moisture (K_q) are determined as:

$$K_{T,q}(z) = \frac{K_m(z)}{P_r} \tag{14}$$

ii) In the free atmosphere

The diffusion coefficient in the free atmosphere over PBL is determined by the local-K approach.

$$K_{m,T}(z) = 1 + l^2(z) f_{m,T}(z) |\frac{\partial U}{\partial z}| \tag{15}$$

where, $l(z)$ is the mixing length given by:

$$\frac{1}{l(z)} = \frac{1}{kz} + \frac{1}{\lambda_{sfc}} \tag{16}$$

which can be rewritten as,

$$l(z) = \frac{ks\lambda_{sfc}}{\lambda_{sfc} + kz} \tag{17}$$

Here, $\lambda_{sfc} = 150m$.

$f_{m,T}(z)$ which appears in equation 15 is the stability function given by:

$$f_{m,T}(z) = \frac{1 + 8(-R_{iB}(z))}{1 + a_1\sqrt{-R_{iB}(z)}} \tag{18}$$

where $a_1 = 1.746$ for momentum and $a_1 = 1.286$ for T and q.

For stable conditions $(R_{iB} > 0)$

$$f_T(z) = \frac{1}{(1 + 5R_{iB}(z))^2} \tag{19}$$

Here, the Richardson number in the free atmosphere is given by:

$$R_{iB}(z) = g\left[\frac{\frac{g}{C_p} + \frac{1}{\overline{T_v}}\frac{\partial T_v}{\partial z}}{\left(\frac{\partial U}{\partial z}\right)^2}\right] \tag{20}$$

$R_{iB}(z)$ has lower bound of -100.0 for very weak wind shear conditions. For unstable conditions, $K_m(z)$ and $K_T(z)$ are determined from equation 15. For stable conditions,K_T is determined from equation 15 but $K_m(z)$ is determined in the following manner:

$$K_m(z) = (K_T(z) - 1)P_r(z) + 1 \tag{21}$$

and Prandtl number is given by:

$$P_r(z) = 1.5 + 2.1R_{iB}(z) \tag{22}$$

The computed diffusion coefficients are bounded between 1 and 1000 m^2s^{-1}.

After having determined the diffusion coefficients, the diffusion equation given in (1) is solved to obtain the tendencies of temperature, specific humidity and momentum.

4. Results

We refer to the model results of M2000 as the control and SSiB for results from the RSM coupled to the SSiB. The comparisions between the two models will be made as far as possible with available observations. In the absence of observations we only emphasize the reasons behind the different features exhibited by the model. Although the model integrations are evaluated in terms of the two seasons of Jan-Feb-Mar (JFM) and Mar-Apr-May (MAM), we shall refer to only one season unless there is a significant change in the relative behaviour of the models from one season to the other. But before we proceed to present the results from these model simulations we first want to show that the implementation of SSiB in RSM is stable and energy conserving. In Figs. 2a(b) we show the difference between the vertically integrated tendency of vertical temperature (moisture) diffusion and the sensible (latent) heat flux from SSiB after 24 hours of the model integration respectively. We note that the difference is very small indicating that mass is conserved in the coupling. This is an important component of the coupling of atmospheric model to the land-surface scheme. In Figs. 3a and b we illustrate the average residue from January through May of 1998 of the surface heat and moisture balance equation from the SSiB integration. We see that the residual is very small thereby showing further evidence that the formulation and implementation of the SSiB and its coupling to the RSM atmosphere is stable.

a) Outgoing longwave radiation

As in the previous paper (M2000) we have looked into the variance of the outgoing long-wave radiation (OLR) anomalies at the intra-seasonal (30-60 days) and high frequency (3-30 days) scales. Observational studies (e.g.Paegle and Mo, 1997) have shown that there is strong telecon-nection between convection over subtropical South America with tropical convection in the eastern

Pacific. Furthermore, this teleconnection has important implications on the predictability of precipitation over the South Atlantic Covergence Zone (SACZ) region. M2000 indicated that there is significant change in the statistics of the weather over continental South America in going from one phase of the ENSO to another.

i) Intraseasonal variability

In Fig. 4 we show the JFM seasonally averaged variance of 30-60 day OLR anomalies from the control, observations (Liebmann and Smith, 1996) and the SSiB runs. It is apparent from the figures that there is an improvement in the simulation of the SACZ at the intraseasonal scales from the SSiB run over the control. Furthermore, the SSiB run shows increased variance over the Nordeste region in north east Brazil in 1997 and 1999 (Figs. 4c and i) as in the observations. Over Amazon River Basin (ARB), there is a slight reduction of variance in the SSiB run relative to the control. However, the variance of the OLR anomalies in the rest of the domain in the two models for all three years are nearly the same.

ii) High frequency variability

In a similar manner we also examined the variance of the high frequency OLR anomalies from the two models. The results of this comparison for JFM is presented in Figs. 5a-i. Once again we see that the largest impact of the SSiB implementation in these regional climate simulations is in the subtropical latitudes of South America and in the SACZ region. Although the SSiB run systematically displays an increased variance in all the three simulations, in the SACZ region it is still less than the observations. As with intra-seasonal anomalies, the high frequency anomalies of OLR from the coupled SSiB simulations also show a tendency for slight reduction in the ARB region compared to the control runs.

b) Precipitation

In Figs. 6a-f the seasonal mean precipitation for both seasons JFM and MAM averaged over

all three simulations of 1997, 1998 and 1999 are shown from the SSiB run, observations (Xie and Arkin, 1994) and control. The improved simulation of precipitation over SACZ region in the SSiB run over control is obvious. The simulation over the Nordeste region in Brazil which was simulated to be erroneously very dry by the control model (Figs. 6c and f) is now wetter in the SSiB runs (Figs. 6a and d). This improved simulation also results in a better simulation of the strong horizontal gradient of precipitation prevalent in this coastal region. Despite the differences observed in variance of OLR at intraseasonal and high frequency scales over the ARB region, the total precipitation bears a strong resemblance between the two models. The characteristic orientation of the precipitation band in the range of 8-16 mm day^{-1} from northeast Brazil to the northwest corner of ARB is very similar in both model simulations. We find that this orientation of the precipitation over the region is very similar to the orientation of the soil wetness (not shown) prescribed initially from National Center for Environmental Prediction (NCEP) reanalysis and maintained through the integration by both models. It is also important to mention here that both the control and the SSiB runs have a tendency to erroneously produce a strong double intertropical convergence zone (ITCZ) in both ocean basins. As in M2000, we also examined the probability density function (pdf) of the precipitation (see Figs. 13 and 14 in M2000) in the SSiB runs (not shown). We found that the pdf of precipitation and its interannual variability in the two models were very similar even over SACZ. This consistency in two different versions of the model further supports our earlier conclusion made in M2000 that the interannual variability of precipitation over South America is accompanied by a change in the number of days of heavy precipitation.

c) Surface Temperature

In Figs. 7a-i we show the surface temperature from the control, observations (Ropelewski et al. 1985) and SSiB runs. The resolution of the gridded surface temperature observations is around 300km. The blank spaces over land in the observations indicate that no verification data were

available in the region. The simulation of the surface temperature from the SSiB runs over the ARB can be seen as a improvement over the cold bias of around 2-4 °C in the control. However, the warm bias over subtropical regions of the Pampas and in the Gran-Chaco area are exaceberated in the SSiB runs. The NCEP reanalysis surface temperatures (not shown) also exhibited a similar warm bias over this region. However the amplitude of this bias is further amplified in the SSiB simulations. Besides the biases mentioned in the lateral boundary conditions, it is found that SSiB relative to other land surface schemes has a tendency to partition the total energy at the surface with higher sensible and lower latent heat fluxes (Dirmeyer et al. 2000b). The surface fluxes averaged over all three simulations for the JFM season from both control and the SSiB runs are shown in Fig. 8. The sensible heat flux from the SSiB runs in the subtropics of South America is about 50 Wm^{-2} higher than the control and the latent heat flux is correspondingly less by about the same amount. However, over the Amazon River Basin the SSiB runs exhibit exactly an opposite behaviour relative to the subtropical area. We also examined the downward shortwave flux at the surface in both the models (not shown) and found that they were nearly identical. This leads us to believe that this difference in surface temperature is inherent to the land surface schemes and independent of the coupling to the atmospheric model.

d) Low Level Circulation

The low level jet (LLJ) is a very significant feature of the monsoon system of South America. It serves as a conduit for the supply of moisture into the subtropics from ARB. Observational studies (Wang and Paegle, 1996) indicate that moisture flux uncertainities in subtropical South America in the various analyses is nearly on the order of 50%. They find that this uncertainty is largely contributed from the wind component due to the substantially different LLJ in the different analyses.

In Figs. 9a-i we show the seasonally averaged (JFM) wind field superposed over the height

field at 850 hPa from the control, NCEP reanalysis and the SSiB runs. The largest differences in the height field between the two versions of the RSM can be seen over the subtropical high in the south Atlantic (SHSA). The SHSA is more elongated to the west in the control relative to the SSiB runs. This results in a stronger pressure gradient to the east of the Andes in the control (Figs. 9a, d and g). In the SSiB runs there is a relatively stronger onshore zonal flow from the tropical Atlantic into the Nordeste region. This can be viewed as a consequence of the increased height gradients apparent in the SSiB runs (Figs. 9c and f) relative to the control (Figs. 9a and d) over the tropical Atlantic in the SSiB runs. The interannual variability of the LLJ is very similar in both the models. In 1998, the LLJ is stronger than in 1999. This is primarily due to the variability of the SHSA which reduces the height/pressure gradient to the east of the Andes in 1999 relative to 1998. However, in comparing the SSiB runs of 1998 (Fig. 9f) and 1999 (Fig. 9i), the enhanced onshore zonal flow from the tropical Atlantic in 1998 is forced to become southerly by the eastern slopes of the Andes mountains. This serves to compensate for the reduced pressure gradient over subtropical South America relative to the corresponding control run (Fig. 9d) to maintain the increased strength of the LLJ in 1998. Because of the coarseness of the NCEP reanalysis shown in Figs. 9b, e and h, it depicts relatively smaller interannual variability of the horizontal pressure gradients to the east of the Andes and over tropical Atlantic and South America. As a result, the interannual variability of the onshore flow over tropical South America and the LLJ is not as robust as in the model simulations.

e) Moisture Budget

From our previous disussion it follows that the low level flow is different in the two models over the South American region. This has implications on the moisture budget over the area. In Figs. 10a-f we show the components of the moisture budget averaged over both JFM and MAM seasons over all three simulations of 1997, 1998 and 1999 for both models over ARB, Gran-

Chaco (GRAN), Pampas (PAM), ITCZ over Atlantic (ITCZ), Nordeste (NOR) and SACZ. The outline of these regions are shown in Fig. 12 of M2000. Furthermore, the difference (diff) in the seasonal means between the two model simulations is also depicted in Fig.10. The moisture flux convergence (MFC) is obtained as a residual in these budget computations. It is clear from the figure that the moisture budget over the tropical areas of ARB and ITCZ over the Atlantic (Figs. 10a and d) has the least difference between the two models. However, further south over GRAN and PAM (Figs. 10b and c) the moisture flux convergence over the JFM and MAM seasons in the SSiB runs are relatively higher than the control by around 1.5 and 1 mm day^{-1} respectively. Over GRAN, this results in a increase in precipitation in both JFM and MAM seasons despite a small reduction in the surface evaporation (SE) relative to the control run. However, over PAM, the increase in moisture flux convergence is not sufficient to offset the decrease in surface evaporation in the SSiB runs, resulting in slightly less precipitation than the control in both JFM and MAM seasons. In the NOR region, the increased intensity of onshore flow in the SSiB model has resulted in not only increased moisture flux convergence but a small increase in surface evaporation as well. This has significantly enhanced the precipitation over the NOR region in the SSiB runs relative to the control. Likewise in the SACZ region, there is a increase in moisture flux convergence and surface evaporation in the SSiB runs relative to the control resulting in more precipitation in the coupled RSM-SSiB model output. The amplitude of this increase diminished in the MAM season.

5. Conclusions

In this paper, we have made an evaluation of the effect of SSiB on the evolving regional climate simulation over South America. This examination was accomplished by comparing a control version of the RSM which had the Mahrt and Pan (1984) land surface scheme with coupled RSM-SSiB model simulations. Amongst the many differences between the two schemes, the most striking is that the control RSM had a homogeneous vegetation and soil distribution while in SSiB there are

12(6) different vegetation (soil) types defined.

The largest differences between the simulated precipitation from the two models were found the SACZ region. The SSiB model showed more precipitation over this region than the control, bringing the model simulation closer to the observations of Xie and Arkin (1996). The variance of the OLR anomalies from the SSiB model at intra-seasonal and high frequency scales also showed a greater similarity to the observed variance from Liebmann and Smith (1994) over the SACZ region. In the rest of the area of the model domain the results were very similar between the two models.

The comparison of surface temperature between the two models revealed that the warm bias of the SSiB model improved the simulation over ARB relative to the control. However, the SSiB model exhibited too warm a surface temperature in the sub-tropical latitudes over Pampas and Gran-Chaco area. This is probably a result of the existence of a similar bias in the driving NCEP reanalysis, and an inherent feature of SSiB to produce higher sensible heat flux and lower latent heat flux for a given atmospheric condition.

The relatively lower latent heat flux and yet higher seasonal precipitation from the SSiB runs over the subtropical region in South America leads us to conclude that the increase in precipitation over these regions is from a increase in moisture flux convergence which not only compensates for decreased surface evaporation but enhances seasonal precipitation over the region. The moisture budget computed over various regions in the subtropics confirmed this conclusion over Gran-Chaco area. However over the Pampas region, the decrease in surface evaporation was slightly higher than in Gran-Chaco resulting in a decrease in the precipitation over the area relative to the control.

On examining the low level circulation we found that the onshore flow from the Atlantic into Nordeste region is enhanced in the SSiB runs. This is a result of the increase in surface pressure gradients in the tropical Atlantic ocean. This increased the moisture flux convergence and surface

evaporation over the Nordeste region relative to the control. Furthermore, despite a decrease in the surface pressure gradient to the east of the Andes in the coupled SSiB integrations of 1998 relative to the control, the strength of the jet in the two models are still comparable. Our conjecture is that the enhanced onshore easterlies which are forced to become southerlies by the eastern slopes of the Andes contribute significantly to the strength of the low level jet in the SSiB run of 1998.

Although we have not discussed in the paper the diurnal variations in the model, we observed that the amplitude and phase of the diurnal signal in precipitation, surface fluxes and surface temperature are nearly identical in both models. Likewise the seasonal anomalies are also very similar in both models.

Although we have compared a regional model with two different land surface schemes, this study is limited by a small sample size of multiseasonal simulations. Furthermore, in the SSiB runs, the lateral boundary conditions are forced by NCEP reanalysis which has a bias towards the Mahrt and Pan (1984) scheme and therefore may reduce the influence of the SSiB scheme on the generated regional climate. We are presently analysing seasonal integrations from this coupled RSM-SSiB model nested into a GCM which has SSiB as its land surface scheme as well. Ultimately, this nested coupled model with identical land surface physics will be used to investigate climate variability over the South American region.

Acknowledgements

We thank Drs. Henry Juang and M. Kanamitsu for giving valuable suggestions and help in implementing the SSiB into RSM. We also acknowledge the useful comments of Drs. David Straus and Adam Schlosser which greatly improved the quality of this report. This project was supported by NASA grant NAG5-8416 and NOAA grant NA86GP0258.

References

Chou, S. C., A. M. B. Nunes and I. F. A. Cavalcanti, 2000: Extended range forecasts over South America using the regional eta model. *J. Geophys. Res.*, **105**, 10147-10160.

Dirmeyer, P. A., 2000a: Using a global soil wetness data set to improve seasonal climate simulation. *J. Climate*, **13**, 2900-2922.

Dirmeyer, P. A. , F. J. Zeng, A. Ducharne, J. C. Morrill, and R. D. Koster, 2000b: The sensitivity of surface fluxes to soil water content in three land surface schemes. *J. Hydrometeor*., **1**, 121-134.

Dirmeyer, P. A. and F. J. Zeng, 1999: An update to the distribution and treatment of vegetation and soil properties in SSiB. COLA Tech. Rep. No. 78. Available from COLA, 4041 Powder Mill Road, Suite 302, Calverton, MD 20705, USA, 25 pp.

Dirmeyer, P. A. and F. J. Zeng, 1997: A two dimensional implementation of the Simple Biosphere (SiB) model. COLA Tech. Rep. No. 48. Available from COLA, 4041 Powder Mill Road, Suite 302, Calverton, MD 20705, USA, 30 pp.

Fennessy, M. J., and J. Shukla, 1996: Impact of Initial Soil Wetness on Seasonal Atmospheric Prediction. COLA Tech. Rep. No. 34. Available from COLA, 4041 Powder Mill Road, Suite 302, Calverton, MD 20705, USA, 31 pp.

Giorgi, F., 1990: Simulation of regional climate using a limited area model nested in a general circulation model. *J. Climate*, **3**, 941-963.

Ji, Y., and A. D. Vernekar, 1997: Simulation of the Asian summer monsoons of 1987 and 1988 with a regional model nested in a global GCM. *J. Climate*, **10**, 1965-1979.

Juang, H.-M., S.-Y. Hong and M. Kanamitsu, 1997: The NCEP Regional Spectral Model: An Update. *Bull. Amer. Soc.*, **78**, 2125-2143.

Juang, H.-M. and M. Kanamitsu, 1994: The NMC Nested Regional Spectral Model. *Mon. Wea. Rev.*, **122**, 3-26.

Kalnay, E. and M. Kanamitsu, 1988: Time Schemes for Strongly Nonlinear Damping Equations. *Mon. Wea. Rev.*, **116**, 1945-1958.

Liebmann, B. and C. A. Smith, 1996: Description of a Complete (Interpolated) Outgoing Longwave Radiation Dataset. *Bull. Amer. Soc.*, **77**, 1275-1277.

Mahrt, L. and H.-L. Pan, 1984: A two layer model of soil hydrology. *Bound.-Layer Meteor.*, **29**, 1-20.

Misra, V., P. A. Dirmeyer and B. Kirtman, 2000a: Regional Simulation of Interannual Variability over South America. Submitted to *J. Geophys. Res.*

Meeson, B. W., F. E. corprew, J. M. P. McManus, D. M. Myers, J. W. Closs, K. J. Sun, D. J. Sunday, and P. J. Sellers, 1995: ISLSCP Initiative I- Global data sets for land-atmosphere models, 1987-1988. Volumes 1-5. Published on CD-ROM by NASA (USA_NASA_GDAAC_ISLSCP_001USA_NASAGDAAC_ISLSCP_005).

Paegle, J., and K. C. Mo, 1997: Alternating Wet and Dry Conditions over South America during Summer. *J. Climate*, **125**, 279-291.

Paegle, J., K. C. Mo and J. N. Paegle, 1996: Dependence of simulated precipitation on surface evaporation during the 1993 United States summer floods. *Mon. Wea. Rev.* **124**, 345-361.

Pereira, L. G. P., M. A. F. S. Dias, A.J.P. Filho and P. T. Matsuo, 2000: Timing of convection initiation during the WETAMC-LAB. Book of abstracts, *First Scientific Conference of the Large Scale Biosphere Atmosphere Experiment in Amazonia*, June 26-30, Belem, Brazil.

Polcher, J. and others, 1998: A proposal for a general interface between land surface schemes and general circulation models. *Global and Planetary Change,* bf 19, 261-276.

Ropelewski, C. F., J. E. Janowiak and M. F. Halpert, 1985: The analysis and display of real time surface climate data. *Mon. Wea. Rev.*, **113**, 1101-1107.

Sellers, P. J., 1985: Canopy reflectance, photosynthesis and transpiration. *Int. J. Remote Sensing*, **6**, 1335-1372.

Sellers, P. J., Y. Mintz, Y. C. Sud and A. Dalcher, 1986: A simple biosphere model (SiB) for use within general circulation models. *J. Atmos. Sci.*, **43**, 505-531.

Tanajura, C., 1996: Modeling and Analysis of the South American Summer Climate. Ph. D.

Dissertation, University of Maryland.

Viterbo, P. and A. K. Betts, 1999: Impact of the ECMWF reanalysis soil water on forecasts of the July 1993 Mississipi flood. *J. Geophys. Res.*, **104**, 19361-19366.

Xie, P. and P. Arkin, 1996: Analysis of global monthly precipitation using guage observations, satellite estimates and numerical model predictions. *J. Climate*, **9**, 840-858.

Xue, Y., F. J. Zeng and C. A. Schlosser, 1996: SSiB and its sensitivity to soil properties - a case study using HAPEX-Mobilhy data. *Global and Planetary Change*, **13**, 183-194.

Xue, Y., P. J. Sellers, J. L. Kinter and J. Shukla, 1991: A simplified biosphere model for global climate studes. *J. Climate*, **4**, 345-364.

Wang, M. and J. Paegle, 1996: Impact of analysis uncertainty upon regional atmospheric moisture flux. *J. Geophys. Res.*, **101**, 7291-7303.

Table 1: List of symbols

Symbol	Units	Meaning
R_{iB}		Richardson number
L	meters	Monin-Obhukov length
h_{pbl}	meters	Height of boundary layer height
R_{iBsfc}		Richardson number in the surface layer
δz_1	meters	Height of the first level of the atmospheric model from surface
k		Vonkermann constant (=0.4)
T_v	Kelvin	Virtual temperature
λ_{sfc}	meters	asymptotic length scale
θ	Kelvin	Potential temperature
θ_r	Kelvin	θ at the reference level (lowest level of the atmospheric model)
θ_v	Kelvin	Virtual potential temperature
θ_{vsfc}	Kelvin	Virtual potential temperature at surface
K_A	m^2s^{-1}	Diffusion coefficient for variable A
u	ms^{-1}	zonal wind
v	ms^{-1}	meridional wind
q		specific humidity
u_*	ms^{-1}	friction velocity
γ_k	[unit of k]m^{-1}	counter gradient term of variable k
C_d		Drag coefficient for momentum flux
U	ms^{-1}	Wind speed

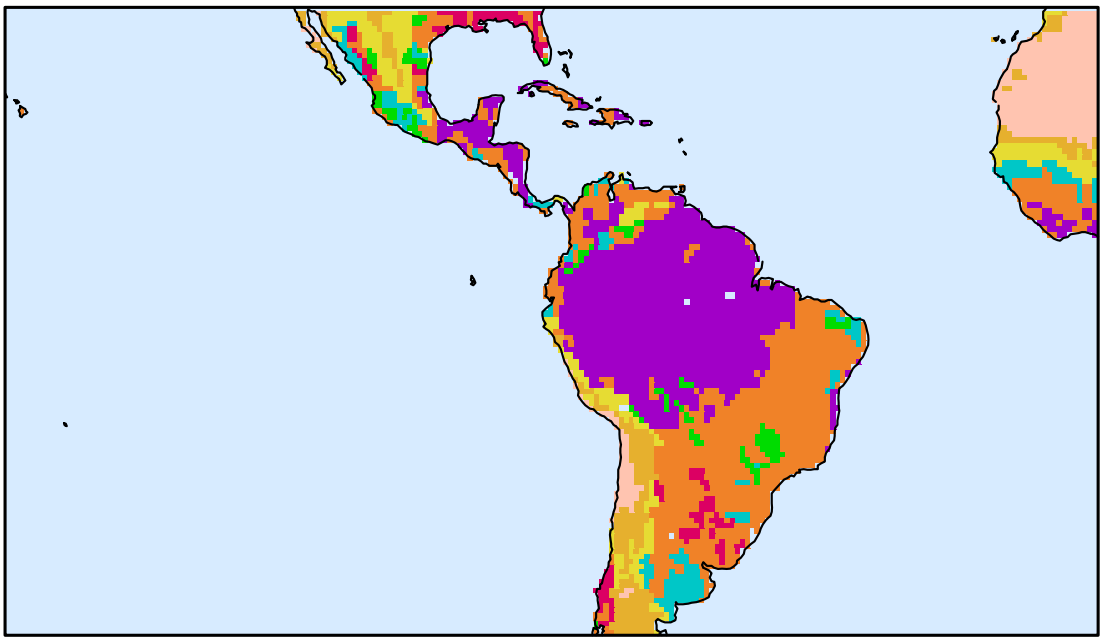

Figure 1: Vegetation types specified from ISLSCP over the domain of integration of the regional model.

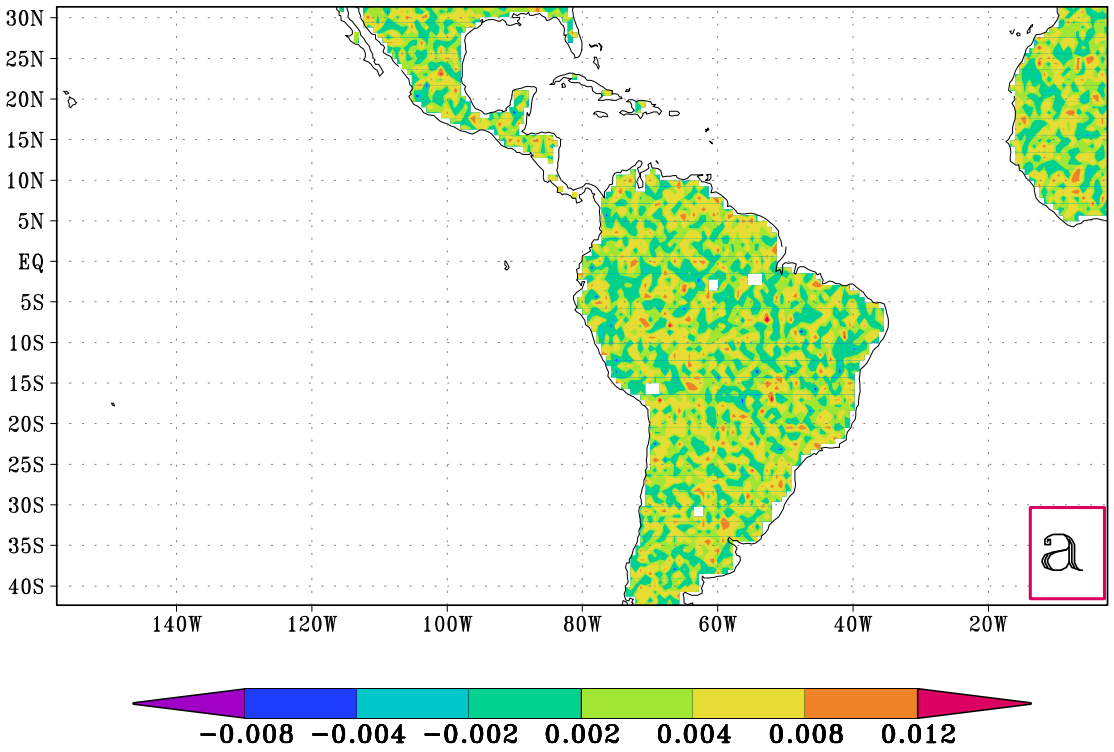

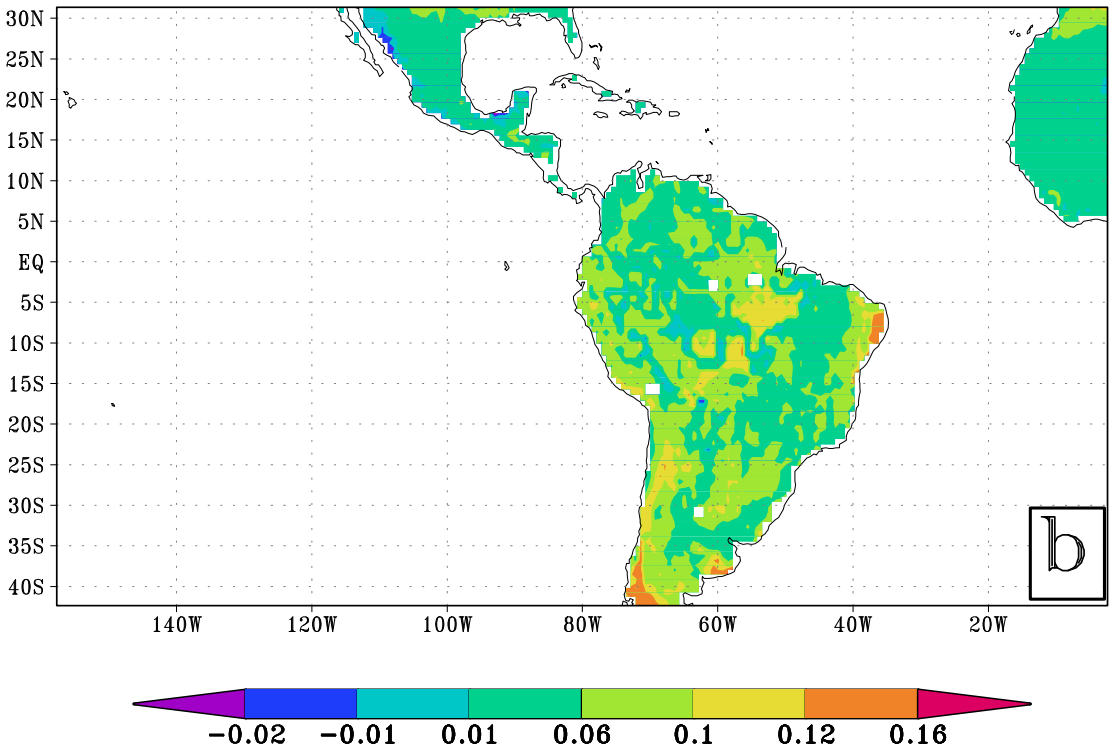

Figure 2: The difference of vertically integrated tendency of a) moisture and b) temperature from vertical diffusion and the corresponding fluxes from SSiB. The units are in Wm^2.

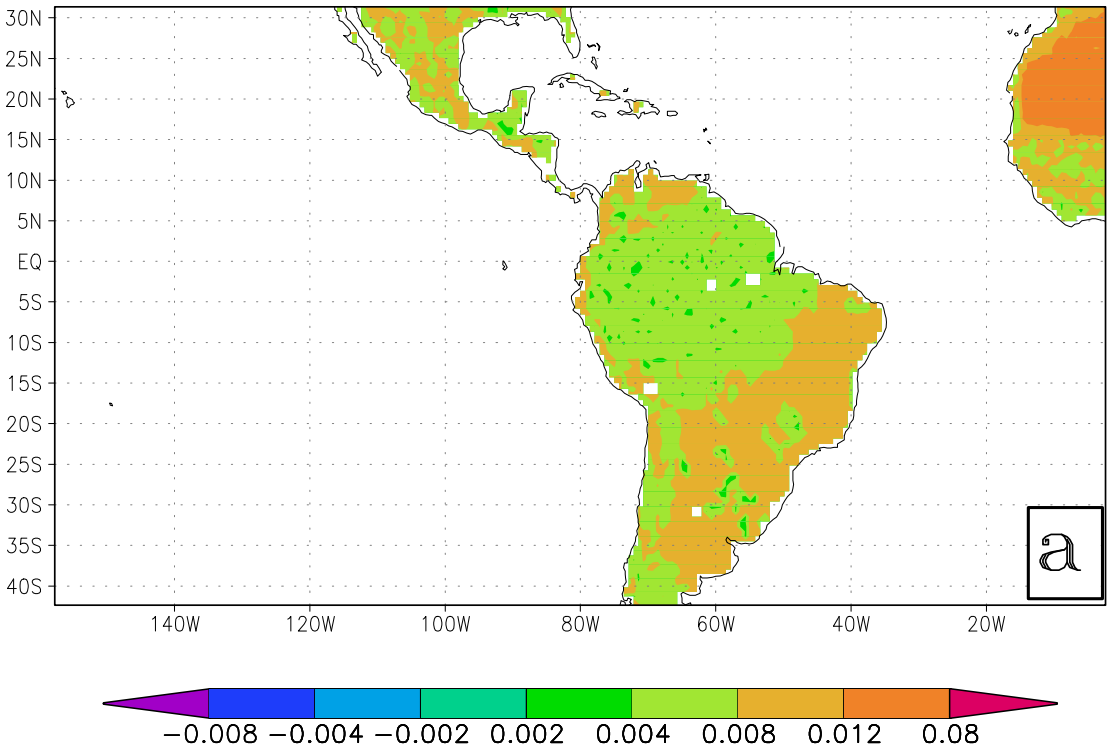

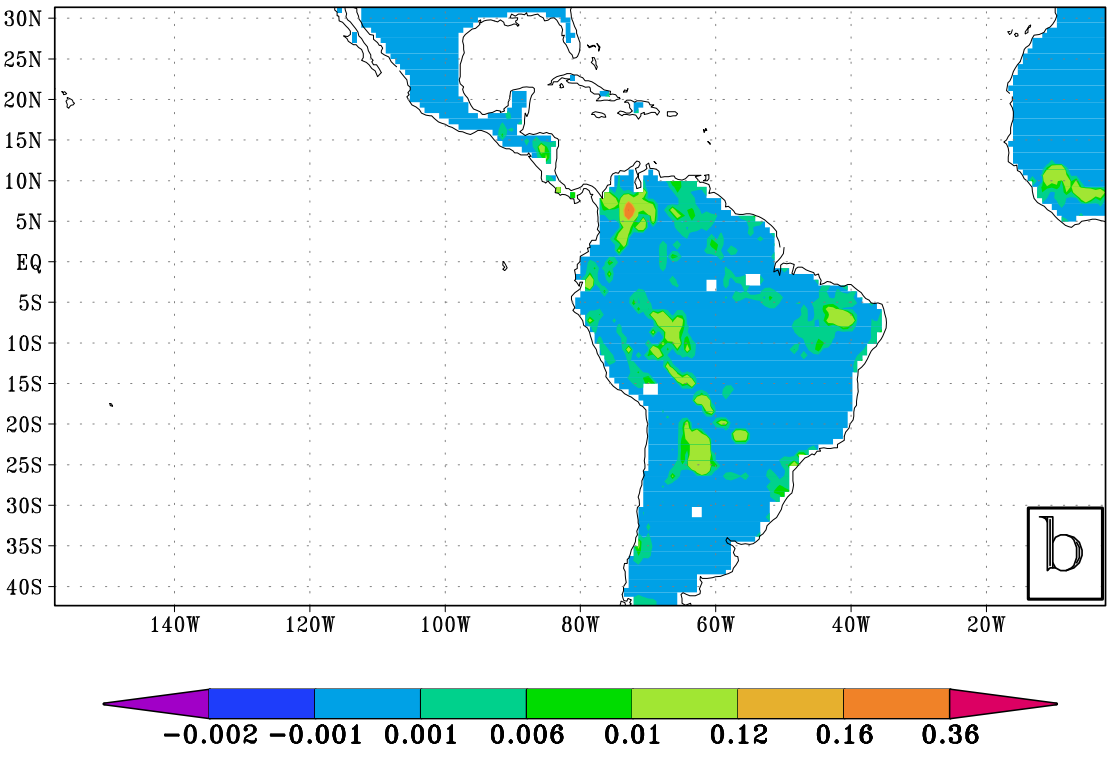

Figure 3: Seasonal (Jan-Feb-Mar-Apr-May) mean of the residue from the surface a) heat (units : Wm^2) and b) moisture (units: mm day-1) balance equation.

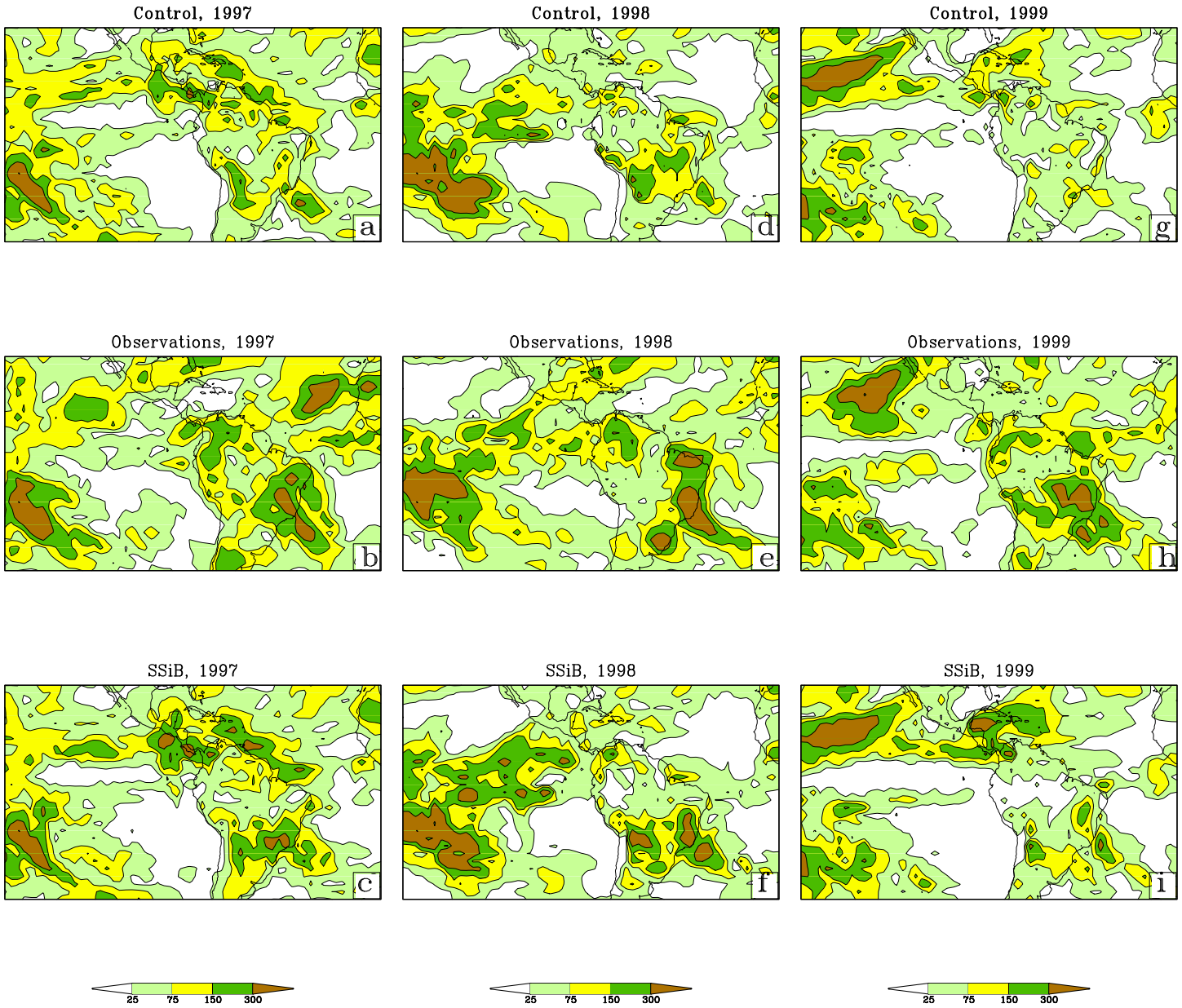

Figure 4: Seasonally averaged variance of 30-60 days OLR anomalies for Jan-Feb-Mar of 1997 from a) Control run, b) Observations and c) SSiB run. Similarly for JFM of 1998 from d) Control run, e) Observations and f) SSiB run and for JFM of 1999 from g) Control run, h) Observations and i) SSiB run. Units are in W^2/m^4.

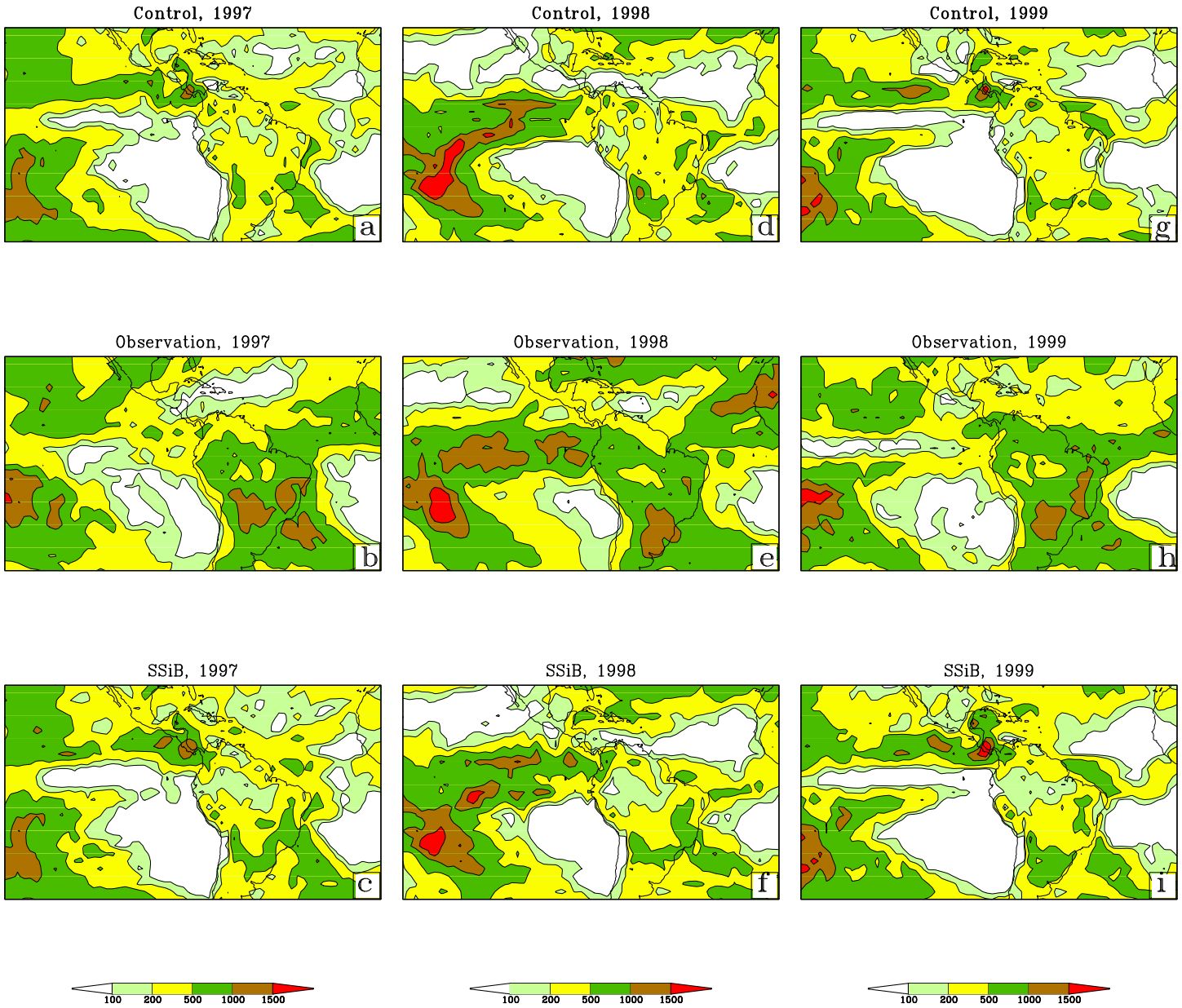

Figure 5: Same as Fig.1 but for OLR anomalies at 3-30 days scale.

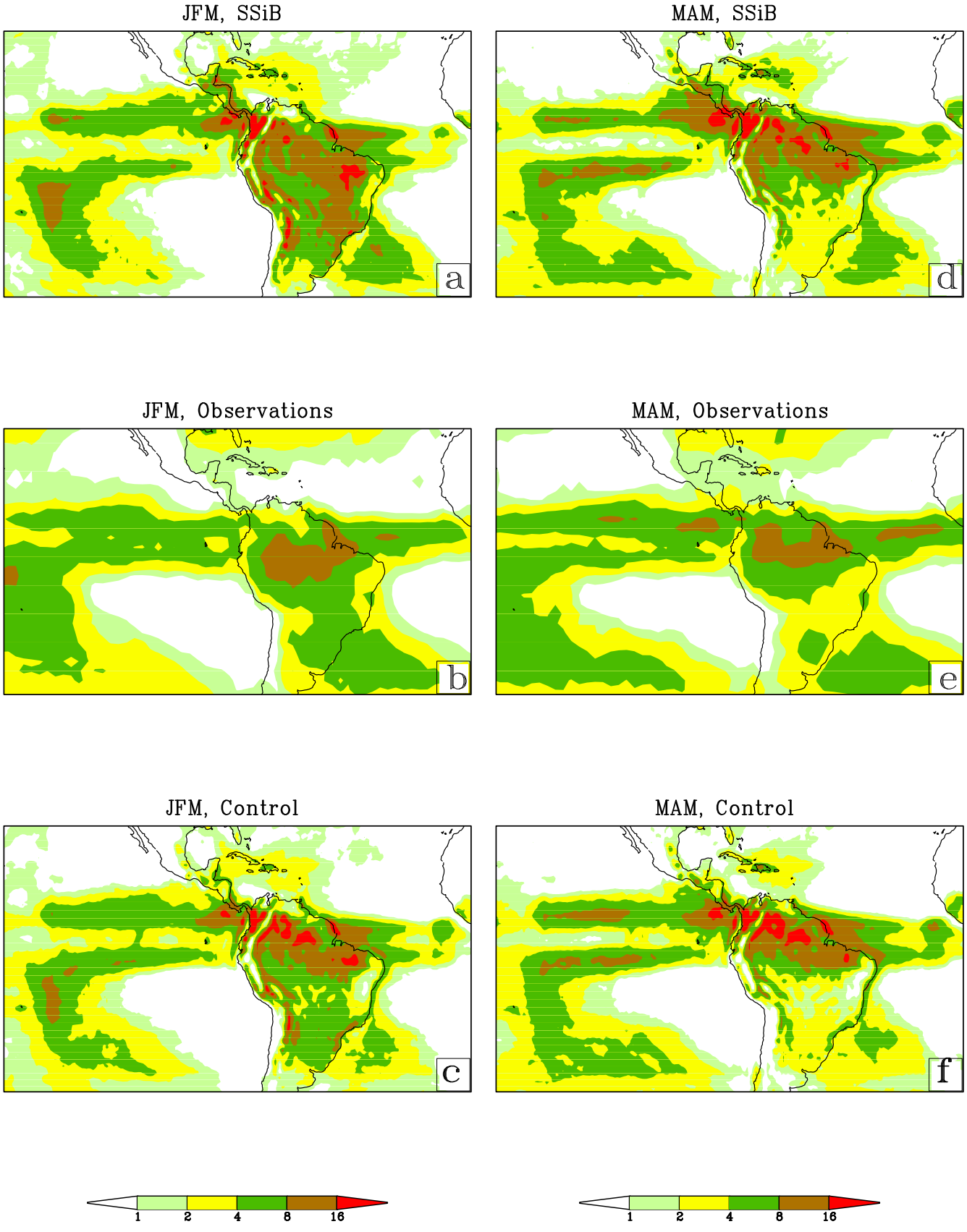

Figure 6: Seasonally averaged (JFM) precipitation over the three model simulations of 1997, 1998 and 1999 from a) SSiB run, b) Observations and c) Control. Similarly, for MAM from d) SSiB run, e) Observations and f) Control. The units are in mm day^{-1}.

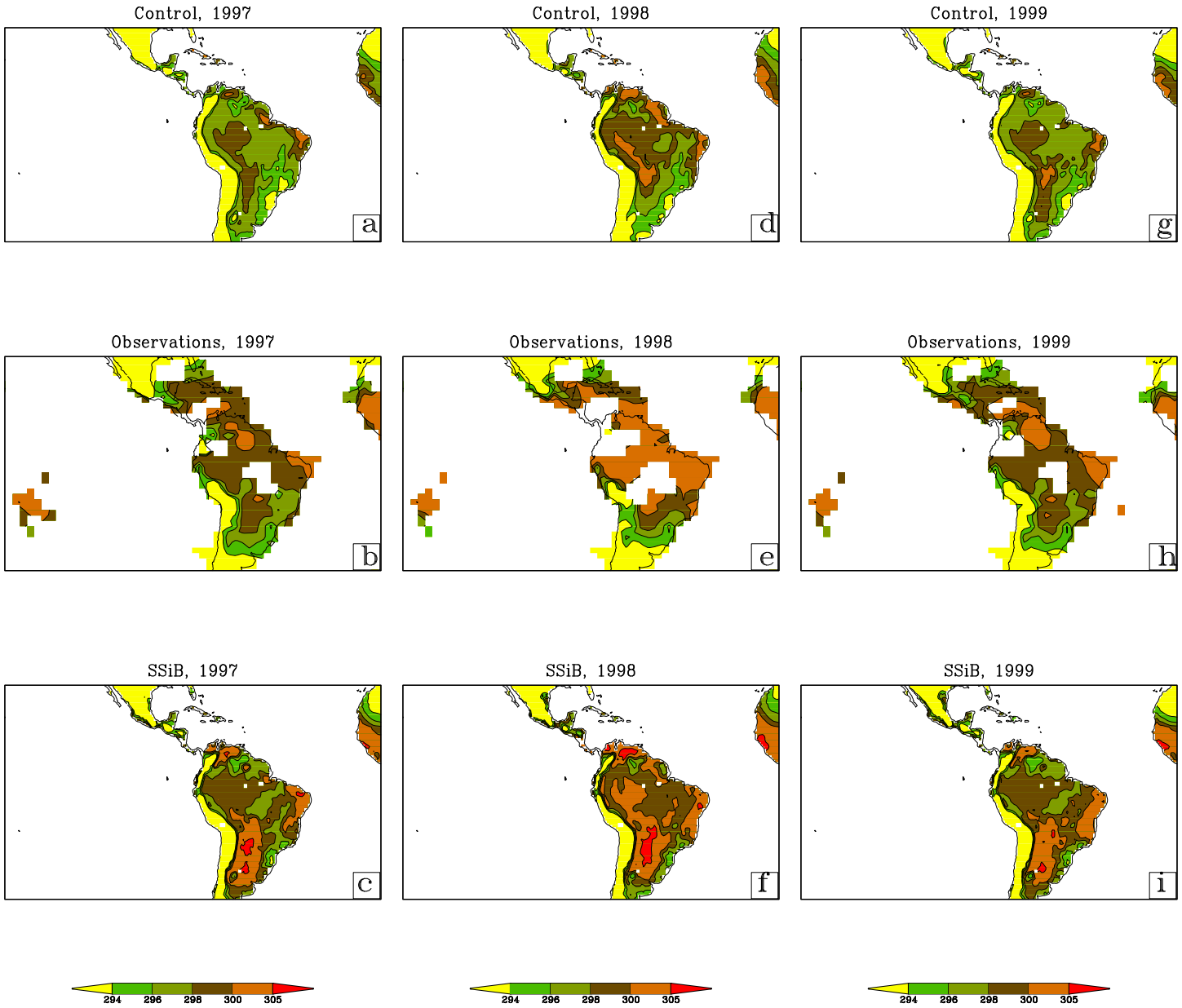

Figure 7: Seasonally averaged (JFM) surface temperature for 1997 from a) Control run, b) Observations and c) SSiB run. Similarly for JFM of 1998 from d) Control run, e) Observations and f) SSiB run and for JFM of 1999 from g) Control run, h) Observations and i) SSiB run. Units are in °C.

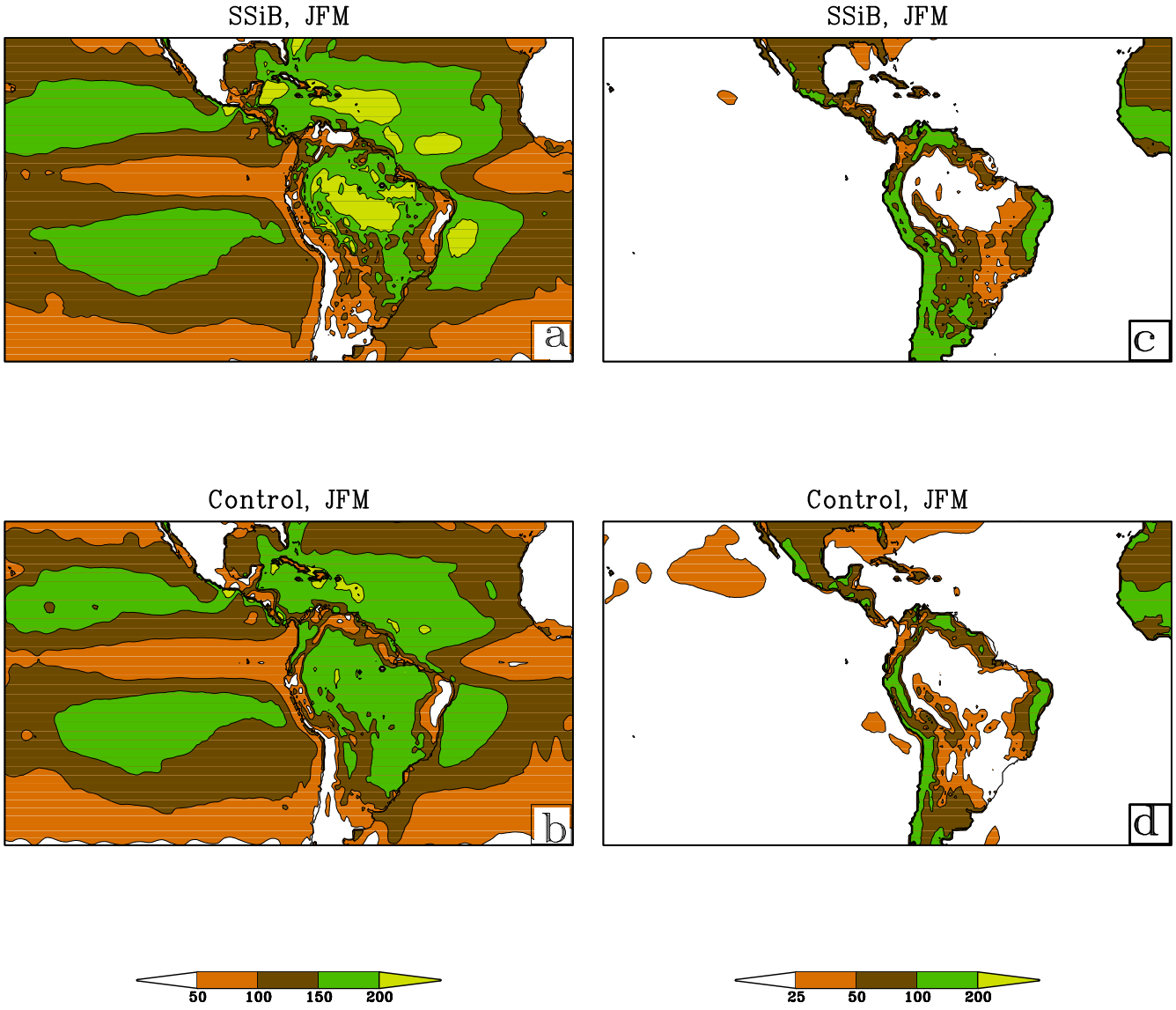

Figure 8: Seasonally (JFM) averaged latent heat flux over all three model simulations of 1997, 1998 and 1999 from a) SSiB run and b) Control. Similarly, for sensible heat flux from c) SSiB run, d) Control. The units are in Wm^{-2}.

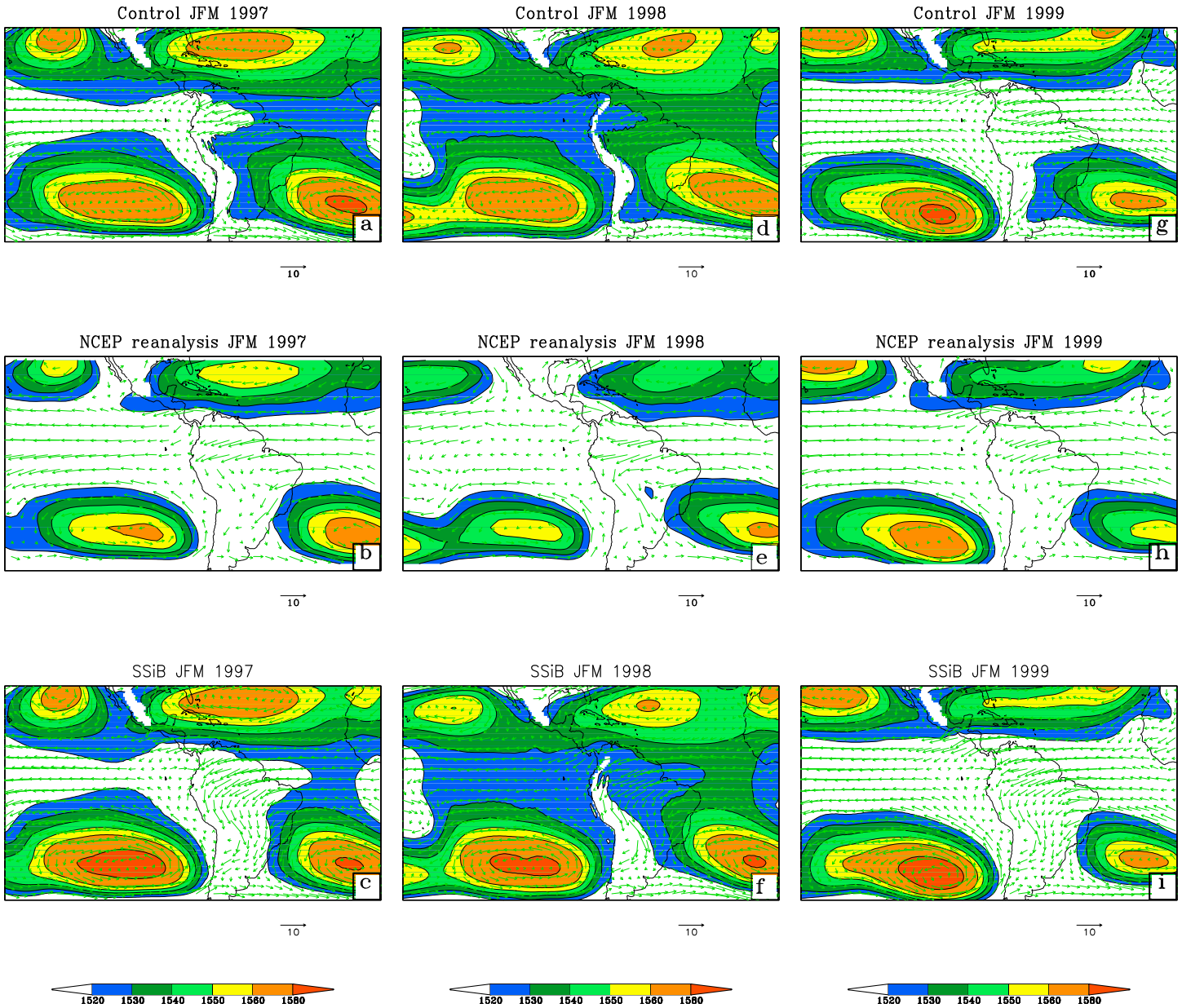

Figure 9: Seasonally averaged (JFM) 850 hPa circulation superposed over 850hPa heights of 1997 from a) Control run, b) Observations and c) SSiB run. Similarly for JFM of 1998 from d) Control run, e) Observations and f) SSiB run and for JFM of 1999 from g) Control run, h) Observations and i) SSiB run. The units of the height field are in m and winds are in m^{-1}.

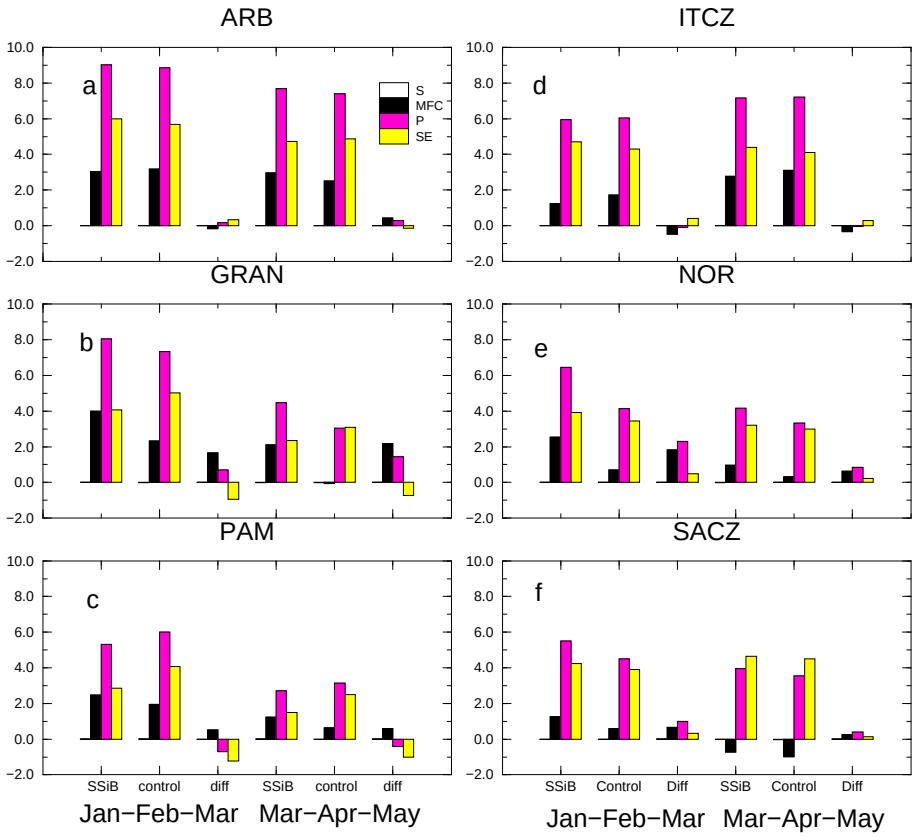

Figure 10: The moisture budget from the control and SSiB versions of RSM averaged over all 3 simulations of 1997, 1998 and 1999 over a) Amazon River Basin (ARB), b) Gran-Chaco (GRAN), c) Pampas (PAM), d) ITCZ over Atlantic (ITCZ), e) Nordeste (NOR) and f) SACZ. The moisture budget components are Storage (S), Moisture Flux Convergence (MFC), Precipitation (P) and Surface Evaporation (SE). ”diff” corresponds to SSiB-control. The units are in mmday^{-1}.